Molecular Properties of Ibuprofen and Its Solid Dispersions with Eudragit RL100 Studied by Solid-State Nuclear Magnetic Resonance

ARTICLE *in* PHARMACEUTICAL RESEARCH · OCTOBER 2005

Impact Factor: 3.42 · DOI: 10.1007/s11095-005-6249-5 · Source: PubMed

5 AUTHORS, INCLUDING:

Marco Geppi
Università di Pisa
120 PUBLICATIONS **1,289** CITATIONS
SEE PROFILE

Giulia Mollica
Aix-Marseille Université
30 PUBLICATIONS **372** CITATIONS
SEE PROFILE

Rosario Pignatello
University of Catania
139 PUBLICATIONS **2,131** CITATIONS
SEE PROFILE

Carlo Alberto Veracini
Università di Pisa
233 PUBLICATIONS **2,359** CITATIONS
SEE PROFILE

Pharmaceutical Research, Vol. 22, No. 9, September 2005 (© 2005)
DOI: 10.1007/s11095-005-6249-5

Research Paper

Molecular Properties of Ibuprofen and Its Solid Dispersions with Eudragit RL100 Studied by Solid-State Nuclear Magnetic Resonance

Marco Geppi,[1,3] Salvatore Guccione,[2] Giulia Mollica,[1] Rosario Pignatello,[2] and Carlo A. Veracini[1]

Received March 24, 2005; accepted May 31, 2005

Purpose. The aim of this study was to investigate, at a molecular level, the structural and dynamic properties of the acidic and sodium salt forms of ibuprofen and their solid dispersions with Eudragit RL-100, obtained by two different preparation methods (physical mixtures and coevaporates), which may affect the release properties of these drugs in their dispersed forms.
Methods. ^{1}H and ^{13}C high-resolution solid-state nuclear magnetic resonance techniques, including single-pulse excitation magic-angle spinning, cross-polarization magic-angle spinning, and other selective 1D spectra, as well as more advanced 2D techniques Frequency Switched Lee-Goldburg HETeronuclear CORrelation (FSLG-HETCOR) and Magic Angle Spinning -J- Heteronuclear Multiple-Quantum Coherence (MAS-J-HMQC) and relaxation time measurements were used.
Results. A full assignment of ^{13}C resonances and precise ^{1}H chemical shift values were achieved for the first time for the two forms of ibuprofen that showed very different interconformational dynamic behavior; drug–polymer interactions were observed and characterized in the coevaporates of the two forms but were much stronger for the acidic form.
Conclusions. A combined analysis of several high-resolution solid-state nuclear magnetic resonance experiments allowed the investigation of the structural and dynamic properties of the pure drugs and of the solid dispersions with the polymer, as well as of the degree of mixing between drug and polymer and of the chemical nature of their interaction. Such information could be related to the *in vitro* drug release profiles observed for the tested coevaporates.

KEY WORDS: ^{1}H and ^{13}C chemical shifts; drug–polymer coevaporates; FSLG-HETCOR; interconformational motions; magic-angle spinning; MAS-J-HMQC; polymorphism; solid-state NMR.

INTRODUCTION

Solid state nuclear magnetic resonance (NMR) is an increasingly important technique for the physical characterization of active pharmaceutical ingredients that allows direct investigation of solid pharmaceutical products (which represent about 80–90% of the market) in their final dosage and dispensed forms, revealing possible physicochemical modifications induced by the processing or manufacturing steps. Indeed, in the last 25 years, solid-state NMR has evolved from the birth of "high-resolution" techniques [thanks to the combination of magic-angle spinning (MAS), cross polarization (CP), and high-power decoupling] to the development of more sophisticated pulse sequences (1), which exploit the availability of significant technological improvements to get specific and detailed information on nuclear properties and, consequently, on the physicochemical behavior of the system under study.

The analysis of standard solid-state high-resolution ^{13}C spectra is extensively used to investigate drug polymorphism (2–5) because of the dependence of nuclear chemical shifts from both chemical structure and conformational and molecular packing behavior. However, solid-state NMR allows a wider range of information to be obtained on pharmaceutical compounds because it can investigate structural and dynamic properties at a molecular level in both crystalline and amorphous phases, as well as the chemical or physical interactions occurring between different domains in complex systems, such as drug–carrier solid dispersions, which can be directly related to the bioavailability of the drug (6). This potential has been only partially exploited in the pharmaceutical field because several solid-state NMR techniques take advantage of technological improvements only recently applied on most commercial spectrometers.

Some solid-state NMR techniques—from ^{13}C and ^{1}H selective spectra to 2D techniques revealing through-bond and through-space ^{1}H–^{13}C connections, from variable-temperature spectra to relaxation time measurements—were applied in the present paper for the investigation of two forms (acid and sodium salt) of ibuprofen (IBU), a widely used nonsteroidal anti-inflammatory drug, and their solid dispersions with Eudragit RL100 (RL), prepared either as physical mixtures or coevaporates. Eudragit Retard polymers

[1] Dipartimento di Chimica e Chimica Industriale, Università di Pisa, Viale Risorgimento 35, 56126 Pisa, Italy.
[2] Dipartimento di Scienze Farmaceutiche, Università di Catania, Viale A. Doria 6, 95125 Catania, Italy.
[3] To whom correspondence should be addressed. (e-mail: mg@dcci.unipi.it)

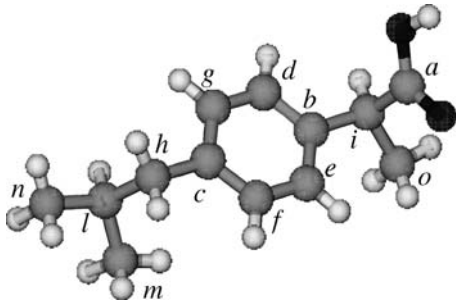

Fig. 1. Structure of IBU-A and labeling of the carbon atoms. For hydrogen atoms, the same labeling used for directly bonded carbons was adopted in the text.

are commonly used in the pharmaceutical technology for coating of solid dosage forms and were recently proposed for the preparation of controlled-release systems, such as micro- and nanoparticles (7–9).

The dissociation state of the active pharmaceutical ingredient (i.e., acid/base or salt form) is important in determining the properties of the dispersed drug, such as bioavailability, stability, ease of manufacture, and therapeutic efficacy. Salt forms of a drug are particularly investigated because they generally exhibit higher physical stability and solubility than the corresponding unionized forms and because of the possibility of widely varying their properties by choosing different counterions. Although the dissociation state of IBU can only marginally affect its therapeutic activity, this aspect assumes great relevance from a formulation point of view, in particular when a solid dosage form is taken into account. Indeed, the peculiar structural and dynamic properties shown at a molecular level by the different forms of IBU are particularly interesting in analyzing the interactions between such forms and a polymeric network in a solid dispersion or a matrix-type drug delivery system, mainly when the polymer itself contains charged moieties. In these systems, electrostatic interactions can arise, depending on the dissociation state of IBU, that affect the affinity between the components and, consequently, the release rate and the pharmacological profile of the active compound (9,10).

The aim of this work was the investigation, by means of solid-state NMR techniques, of the difference in structural and dynamic properties between the acidic (IBU-A) and salt (IBU-S) forms of IBU and between the pure drug and the solid dispersions, as well as of the chemical interactions and the degree of mixing between IBU and RL domains in the different solid dispersions. At first, this required detailed analysis and full assignment of solid-state ^{1}H and ^{13}C spectra that, despite IBU being an extensively studied drug, to the best of our knowledge were never performed before. The information obtained from the analysis of spectral features and 2D and variable-temperature experiments allowed the molecular structural and dynamic behavior to be highlighted. The change in this behavior from pure drugs to solid dispersions and the presence of IBU–RL chemical interactions were investigated by comparison of ^{1}H and ^{13}C spectra, whereas the degree of physical mixing between drug and polymer was estimated from the analysis of ^{1}H spin–lattice relaxation times.

The results obtained from solid-state NMR were compared with the drug release behavior observed *in vitro* from RL coevaporates loaded with IBU-A or IBU-S to confirm how the electrostatic interactions occurring between the drug and polymer can affect the overall physicochemical behavior of this delivery system.

MATERIALS AND METHODS

Samples

Ibuprofen sodium salt (IBU-S, racemic mixture) was purchased from Sigma-Aldrich Chimica Srl (Milan, Italy), and was used as received. The corresponding acidic form (IBU-A) was obtained by treating an aqueous solution of the sodium salt with diluted acetic acid under cooling. The resulting white solid was collected by filtration, washed extensively with water, and freeze-dried. Determination of melting point, thin-layer chromatography, and elemental analysis confirmed the identity and purity of this compound (Merck Index).

The structure of IBU-A, retrieved from the Cambridge Structural Database System (version 5.26, November 2004; CSD System code: IBPRAC) (11,12), using software CONQUEST (version 1.7) (13), is shown in Fig. 1.

The carrier Eudragit RL100 (RL, see Scheme 1) was purchased from Rohm Pharma (Darmstadt, Germany) and was used as received to obtain two kinds of solid dispersions for each form of the drug, coevaporates and physical mixtures, which were obtained by two different mixing methods: the coevaporates were prepared by codissolving drug and polymer (1:3 by weight) in absolute ethanol at room temperature, stirring the mixture for 4–6 h, and then removing the solvent under vacuum in a rotary evaporator at a maximum temperature of 40°C; the physical mixtures were prepared by simply triturating drug and carrier (1:3 by weight) in a mortar without solvent.

NMR Measurements

All the solid-state NMR experiments were performed on a Varian Infinity Plus 400 (Varian, Cernusco sul Naviglio; Milan, Italy) double-channel spectrometer operating at the ^{1}H frequency of 399.89 MHz, and ^{13}C frequency of 100.56 MHz, equipped with two CP-MAS probes for rotors with an outer diameter of 3.2 and 7.5 mm. Both the ^{13}C and ^{1}H 90° pulses were 4.0 and 1.8 μs for the 7.5- and 3.2-mm probes,

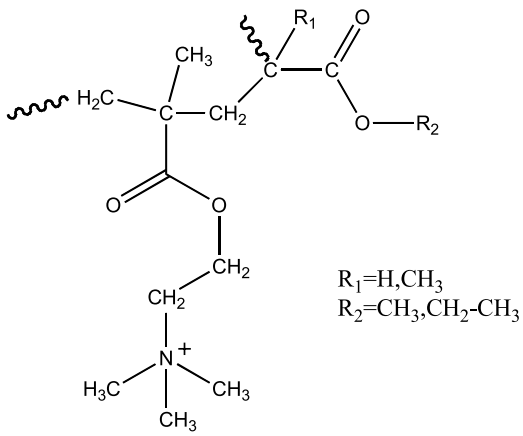

Scheme 1. Chemical structure of Eudragit RL100.

respectively. A relaxation delay of 5 s was used in all the experiments.

A contact time of 1 ms was found to give the maximum signal intensity in the CP experiment for all the samples. Spinning sideband-free ^{13}C spectra were recorded using the total suppression of spinning sidebands (TOSS) technique (14). In the cross polarization–polarization inversion with simultaneous phase inversion (CPPI-SPI) experiment (15), the CP and PI times used to null the methine signals were 42 and 37 μs, respectively. The 2D MAS-J-HMQC technique (16) was used with a contact time of 1 ms, 128 rows, and 400–800 scans; the spinning rate was 10.810 or 7.180 kHz to synchronize the rotation with the pulse sequence timing. The same parameters were applied for all the samples with the 2D HETCOR technique (17), except for a contact time of 300 μs and a spinning rate of 6.600 kHz. ^{1}H spin–lattice relaxation times in the laboratory frame (T_1) measurements were carried out with a ^{13}C-detected inversion–recovery experiment (18). Temperature and MAS spinning rate were always controlled within 0.2°C and 5 Hz, respectively.

In Vitro Dissolution Tests

The drug release from the polymeric matrices was evaluated at room temperature for 24 h. Fifty-milligram samples of each batch were dispersed in 100 mL of phosphate buffer solutions at different pH values (4.5, 7.4, and 9.0) (Italian Pharmacopoeia, FUI X Ed) and stirred at 100 rpm. At predetermined time intervals, 1-mL aliquots of the solution were withdrawn and replaced with fresh buffer. The samples were filtered (0.45-μm polytetrafluoroethylene membrane filters) and the amount of dissolved drug was measured by UV spectrophotometry at 265 nm *vs.* calibration curves obtained for the various drugs at the respective pH.

RESULTS AND DISCUSSION

Pure Ibuprofen

^{13}C Spectra

Several solid-state high-resolution NMR experiments were performed to get a structural characterization of the drugs under investigation. Most information could be obtained from the simple analysis of ^{13}C CP-MAS spectra, reported in Fig. 2.

The relatively small spectral line widths (of the order of 100 Hz) observed for the two IBU forms confirm that they are crystalline, as previously observed by powder X-ray diffraction analysis (PXRD) (10). Moreover, the presence of several resonances less than or equal to the number of inequivalent carbon nuclei in the molecules suggests that, for both the drug forms, a single crystalline form is present and a single independent molecule is in the unit cell. This is in full agreement with previous X-ray structural studies on the racemic form of IBU-A (19).

The discrimination among central "isotropic" peaks and spinning sidebands (occurring at a distance greater than the MAS spinning frequency from the central peaks) was possible by recording both variable spinning rate and TOSS spectra (not shown).

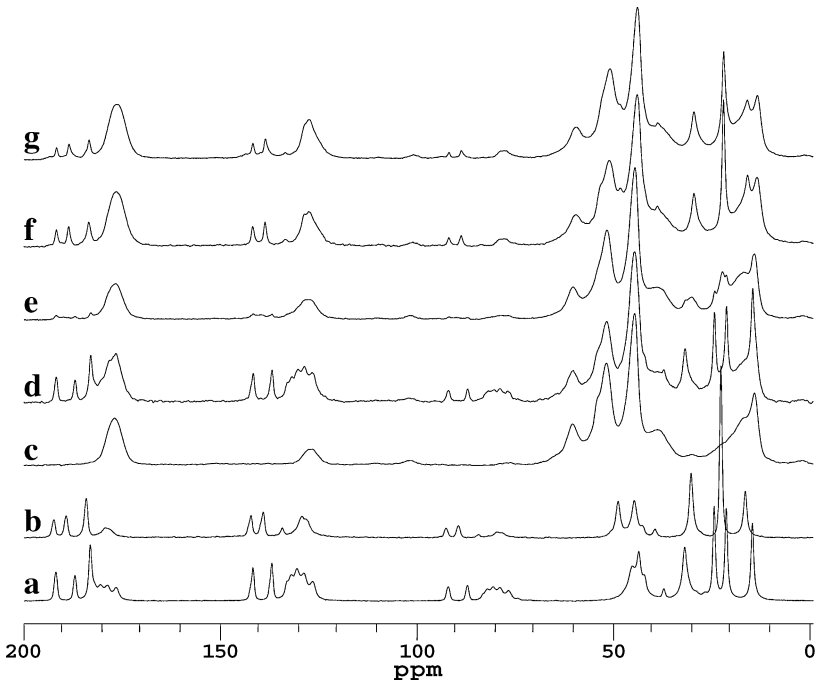

Fig. 2. ^{13}C CP-MAS spectra of (a) IBU-A, (b) IBU-S, (c) Eudragit RL, (d) IBU-A/RL physical mixture, (e) IBU-A/RL coevaporate, (f) IBU-S/RL physical mixture, (g) IBU-S/RL coevaporate. All the spectra shown in this figure were recorded at 25°C and at a spinning rate of 5 kHz. However, several spectra at different spinning rates were also recorded (not shown) to remove the superposition between some isotropic peaks and spinning sidebands.

Table I. Assignment of ^{13}C Solid-State Spectra for IBU-A and IBU-S

^{13}C nucleus	Chemical shifts (ppm)	
	IBU-A	IBU-S
a	183.2	184.2
b	137.2	142.5
c	142.0	139.4
d	132.3	126–133
e	126.7	
f, *g*	129.0, 130.8	
h	46.0	45.3
i	44.2	49.4
l	32.6	31.0
m	25.1	23.4
n	22.0	
o	15.4	17.2

Refer to Fig. 1 for the labeling of the ^{13}C nuclei.

The assignment of the ^{13}C spectral resonances of IBU-A to the different nuclei, reported in Table I, could be in part performed on the basis of the ^{13}C solution spectrum, because the solid-state chemical shifts are usually quite similar, the only differences arising from conformational and/or packing effects. However, the registration of some 1D selective spectra and of 2D correlation maps, reported in the following paragraphs, allowed not only the assignments that could be extrapolated from the solution spectrum to be confirmed, but also several uncertain attributions to be unraveled.

It must be noted that the signals at 25.1 and 22.0 ppm in the solid-state spectrum of IBU-A correspond to the two methyl carbons of the isobutyl group, which are magnetically equivalent in the ^{13}C solution spectrum because of the fast rotation about the CH_2–CH axis. A similar situation is present for the aromatic tertiary carbons, for which four distinct resonances are present in the solid-state spectrum (126.7, 128.8, 130.8, and 132.4 ppm) instead of the two resonances shown by the solution spectrum. The inequivalence in the solid state must be associated to the restricted motional behavior: the isobutyl and phenyl groups are substantially "frozen" in a definite conformation and the different peaks are due to the different chemical environments felt by the two components of the *m–n*, *d–e*, and *f–g* carbon nuclei pairs. This point will be discussed with more detail in the "Variable-Temperature ^{13}C CP-MAS spectra" section.

The signals of methylene and methine carbons could be discriminated by the CPPI pulse sequence on the basis of their different CP dynamics. Indeed, if the peak at 32.6 ppm safely corresponds to the tertiary carbon *l*, those heavily superimposed at 46.0 and 44.2 ppm could not be individually assigned to carbons *h* and *i* on the basis of the sole comparison with the solution spectrum, where indeed they coincide. On the basis of the CPPI experiment, the resonance at 46.0 ppm was assigned to the secondary carbon *h* (see Fig. 3).

From the comparison of the ^{13}C CP-MAS spectra of IBU-A and IBU-S (see Fig. 2a, b), three main differences can be observed concerning the resonances of the methyl carbons of the isobutyl group and of the tertiary aromatic carbons, as well as the group of resonances in the 40- to 50-ppm region. The resonances of the methyl carbons *m* and *n*, which are clearly separated in the spectrum of IBU-A, are coincident in that of IBU-S, reproducing the behavior of the solution spectrum: this must be ascribed to a higher mobility of the isobutyl group that, in IBU-S, is not frozen in a single conformation, but it can rotate around the CH–CH_2 bond so fast that NMR can only reveal an averaged situation. A similar situation is present for the signals arising from tertiary aromatic carbons: the reduction from four to two distinct resonances in the ^{13}C spectrum on passing from IBU-A to IBU-S is due to the occurrence of a fast rotation of the phenyl group about its *para* axis.

Concerning the two resonances between 40 and 50 ppm, the assignment to *i* and *h* carbons must be reversed with respect to IBU-A, as revealed by the CPPI experiment (see Fig. 3). Indeed, in IBU-S the high (49.4 ppm) and low (45.3 ppm) frequency peaks are assigned to the CH group close to the carboxylate function (*i*) and to the CH_2 group of the isobutyl function (*h*), respectively. Comparison with IBU-A shows that these differences are mostly due to the presence of the carboxylate function instead of the carboxylic one, which strongly influences the chemical shift of the neighbor-

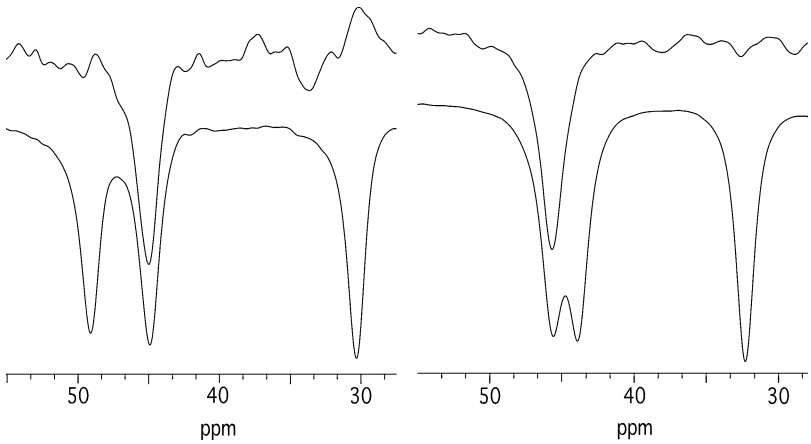

Fig. 3. ^{13}C spectra of IBU-A (right) and IBU-S (left) recorded by the CPPI-SPI pulse sequence (15). The top spectra were recorded with a CP time of 42 μs and a PI time of 37 μs to suppress the tertiary ^{13}C peaks and contain the sole methylene ^{13}C signals as negative peaks. The bottom spectra, recorded with a CP time of 42 μs and a PI time of 1 ms, were used as phase references.

ing carbon *i*, leaving substantially unchanged that of the carbon *h*, which lies on the other side of the phenyl ring within the molecule.

^{1}H Spectra

The ^{1}H MAS spectra of IBU-A and IBU-S, recorded at a spinning rate of 20 kHz, are reported in Fig. 4a, b. In the case of the acidic drug form, three peaks can be distinguished, centered at about 1, 7, and 13 ppm, that can be assigned to aliphatic, aromatic and acidic protons, respectively. The two low-frequency peaks at about 1 and 7 ppm can also be observed in the ^{1}H MAS spectrum of IBU-S, which, however, shows slightly narrower lines, thus suggesting that IBU-S experiences a higher mobility than IBU-A.

Unfortunately, the accessible spinning rates do not allow the ^{1}H–^{1}H homonuclear dipolar interactions to be completely removed by MAS only, and, consequently, a better spectral resolution to be achieved in monodimensional ^{1}H spectra recorded by direct excitation.

2D ^{1}H–^{13}C Correlation Experiments

Additional information was obtained by applying two different ^{1}H–^{13}C 2D correlation techniques: Frequency Switched Lee-Goldburg HETeronuclear CORrelation (FSLG-HETCOR) (17), based on through-space ^{1}H–^{13}C dipolar interactions, and Magic Angle Spinning -J- Heteronuclear Multiple-Quantum Coherence (MAS-J-HMQC) (16), based on through-bonds ^{1}H–^{13}C scalar interactions. Whereas the MAS-J-HMQC experiment can be very useful for a combined interpretation of ^{13}C and ^{1}H spectra, the FSLG-HETCOR technique is more sensitive to long-range couplings and can shed light on conformational and molecular packing aspects of solid samples.

The MAS-J-HMQC maps recorded for IBU-A and IBU-S (see Figs. 5 and 6, respectively) contain the correlations among directly bonded ^{1}H and ^{13}C nuclei. The ^{1}H chemical shift determined from these maps for the different protons are reported in Table II for both samples.

In IBU-A the four tertiary aromatic carbons (125–135 ppm) are correlated to ^{1}H chemical shifts in the range 6.6–8.5 ppm, and the ^{13}C resonances at 132.3 and 126.7 ppm are correlated to higher-frequency ^{1}H signals at 7.6 and 8.5 ppm, respectively, and those at 130.8 and 129.0 ppm with a ^{1}H peak at 6.5–6.6 ppm. As far as the aliphatic resonances are concerned, the correlation peaks relative to the different carbon nuclei can be clearly distinguished. In particular, it must be noted that the ^{13}C peak at 46.0 ppm (carbon *h*) gives two distinct correlation peaks of similar intensity to ^{1}H signals at 2.1 and 2.7 ppm, suggesting that the two protons of the CH_2 group are strongly inequivalent.

In IBU-S, the correlation peaks relative to the aromatic nuclei are missing: these correlation peaks were never revealed in a number of experiments performed by varying the values of several acquisition parameters (spinning rate, contact time, frequency in the ^{1}H dimension, etc.). Therefore, this effect must probably be ascribed to the mobility of the aromatic group, which also gives rise to a lower CP efficiency than in IBU-A. On the contrary, the correlation peaks relative to the aliphatic nuclei are very intense and well separated from each other: in this case the two protons of the CH_2 group resonate at the same frequency, thus suggesting that the inequivalence observed in IBU-A is no longer present in IBU-S because of interconformational mobility.

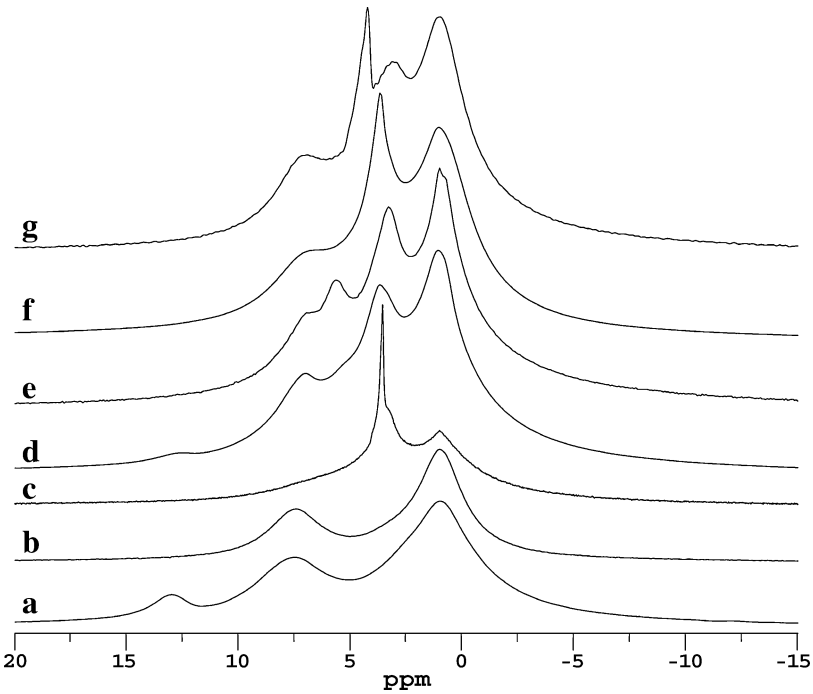

Fig. 4. ^{1}H MAS spectra of (a) IBU-A, (b) IBU-S, (c) RL, (d) IBU-A/RL physical mixture, (e) IBU-A/RL coevaporate, (f) IBU-S/RL physical mixture, and (g) IBU-S/RL coevaporate. All the spectra were recorded at 25°C and at a spinning rate of 20 kHz.

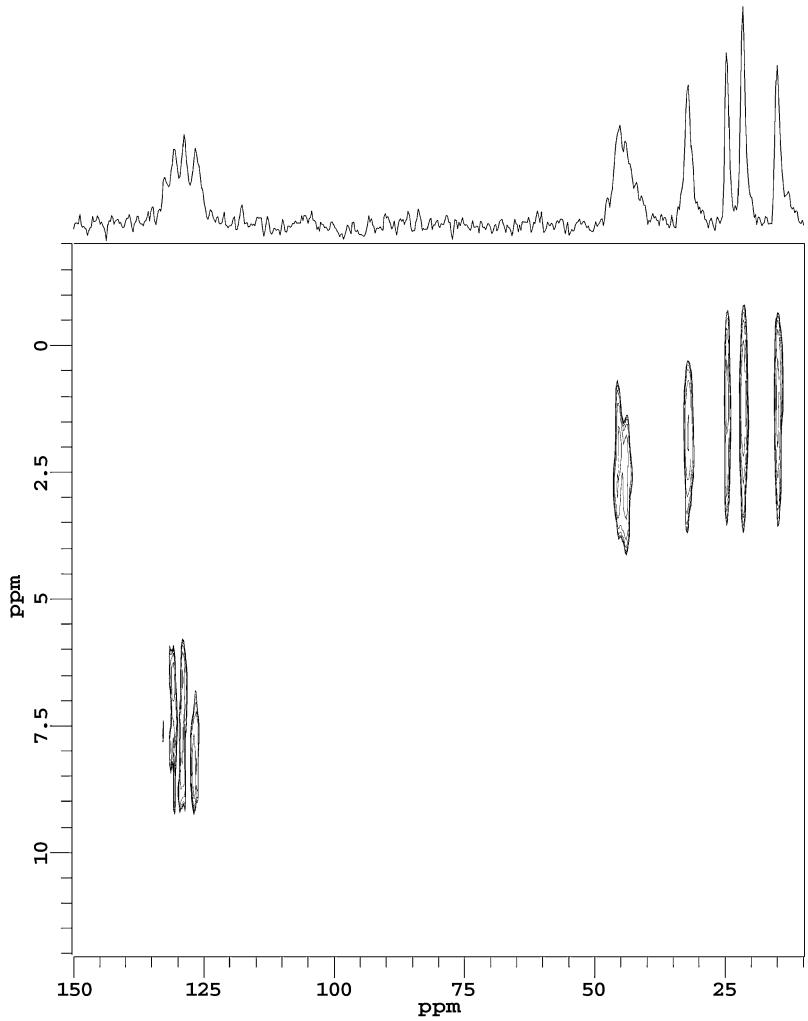

Fig. 5. 2D MAS-J-HMQC map of IBU-A recorded with a spinning rate of 10.810 kHz.

The HETCOR maps obtained for IBU-A and IBU-S, recorded using short CP contact times to minimize spin-diffusion effects, are reported in Figs. 7 and 8, respectively. The most intense correlation peaks are ascribable to directly bonded ^{1}H–^{13}C couples and therefore coincide with the peaks observed in the MAS-J-HMQC maps. However, several peaks with a lower intensity can be revealed in the maps, which arise from coupling among unbonded ^{1}H and ^{13}C nuclei. These correlation peaks were used to perform a more detailed attribution of ^{13}C aromatic resonances.

In IBU-A, carbon *a* shows a double correlation with the acidic proton (~13 ppm) and with proton *i*, bonded to the adjacent methinic carbon. The observation of a strong correlation peak for the acidic proton with the ^{13}C signal at 183.2 ppm is in agreement with the presence of dimeric structures, where such proton is strongly coupled with the carboxylic carbons of the two crystallographically equivalent molecules forming the dimer. The two aromatic quaternary carbons at 137.2 and 142.0 ppm are respectively coupled to the methinic proton *i* (singlet) and to the methylene protons *h* (doublet); therefore they have been assigned to carbons *b* and *c*, respectively. Among tertiary aromatic carbons, the one resonating at 126.7 ppm shows a quite different correlation to directly bonded protons, as previously seen from the MAS-J-HMQC experiment; since cross peaks at the same proton frequency are also observed for carbons *o* and *b*, the ^{13}C peak at 126.7 ppm could be safely assigned to carbon *e*. Moreover, the ^{13}C nuclei resonating at 129.0 and 130.8 ppm behave very similarly and, in particular, are coupled to protons *h*, thus indicating that these resonances arise from carbons *g* and *f*. This assignment of aromatic resonances is further supported by the different cross peaks observed for the quaternary carbons *b* and *c* with aromatic protons.

The HETCOR map of IBU-S is less detailed, especially in the aromatic region, in agreement with the lesser number of peaks observed in the ^{13}C 1D spectra due to the presence of interconformational mobility. However, analysis of the specific correlations among aliphatic protons and aromatic carbons reveals that not only the assignment of carbons *i* and *h* (previously performed on the basis of the CPPI experiment), but also that of carbons *b* and *c* (corresponding to the peaks at 142.5 and 139.4 ppm, respectively) must be reversed with respect to IBU-A (137.2 and 142.0 ppm, respectively). It must be noted that in this case the nature of the "doublet" structure of the peak at 49.4 ppm (assigned to carbon *i*) is different from that of the peak at 46.0 ppm in

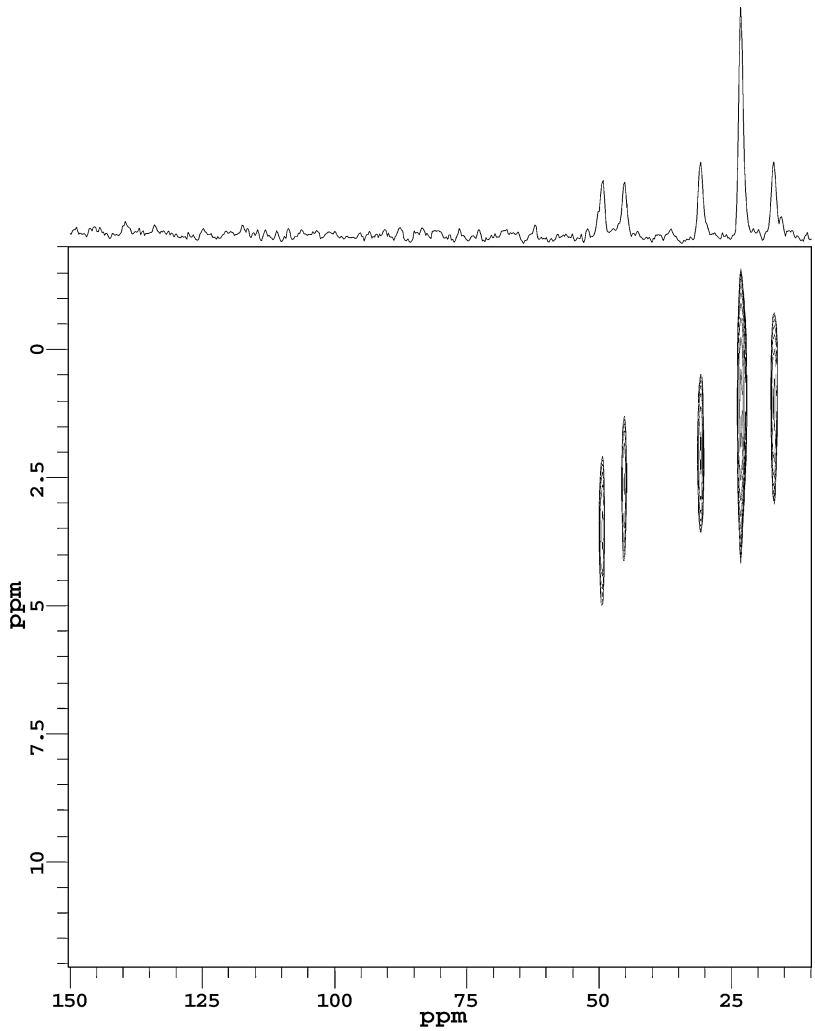

Fig. 6. 2D MAS-J-HMQC map of IBU-S recorded with a spinning rate of 7.180 kHz.

IBU-A assigned to carbon *h*. Indeed, for the latter the doublet was ascribed to the anisochrony of the two directly bonded protons, which could also be observed in the HMQC experiment, whereas for IBU-S such structure is not observed in the HMQC experiment and is therefore due to dipolar couplings to both the directly bonded proton and the neighboring methyl protons, as further confirmed by the presence of a correlation between carbon *o* and proton *i*. The carboxylate ^{13}C nucleus shows a superposition of correlation peaks, wherein three maxima can be distinguished: two of them correspond to *i* and aromatic protons, and the third, relative to a very broad peak, at an intermediate chemical shift, does not correspond to any resonance in the IBU-S molecule. However, given the remarkable amount of water (13.7% by weight) present in the commercial sample, it is possible to explain this peak with the presence of water molecules in the proximity of the carboxylate groups.

Table II. Values of ^{1}H Chemical Shifts Determined from the Correlation Peaks in the MAS-J-HMQC Experiments

IBU-A		IBU-S	
Chemical shift, ^{13}C (ppm)	Chemical shift, ^{1}H (ppm)	Chemical shift, ^{13}C (ppm)	Chemical shift, ^{1}H (ppm)
15.4	1.0	17.2	1.0
22.0	1.2	23.4	1.1
25.1	1.1	31.0	2.0
32.6	1.8	45.3	2.6
44.2	2.6	49.4	3.6
46.0	2.1 and 2.7		
126.7	8.5		
129.0	6.5		
130.8	6.6		
132.3	7.6		

Variable-Temperature ^{13}C CP-MAS Spectra

We have already pointed out in the "^{13}C Spectra" section that some differences (and particularly those relative to the tertiary aromatic and primary isobutylic carbons) between the room temperature ^{13}C spectra of IBU-A and IBU-S must be ascribed to their different dynamic behavior, especially concerning the interconformational jumps about the phenyl *para* axis and $CH–CH_2$ bond in the isobutyl group. The presence of a single peak for methyl carbons *m* and *n* in IBU-S indicates that fast rotations about the $CH–CH_2$ bond

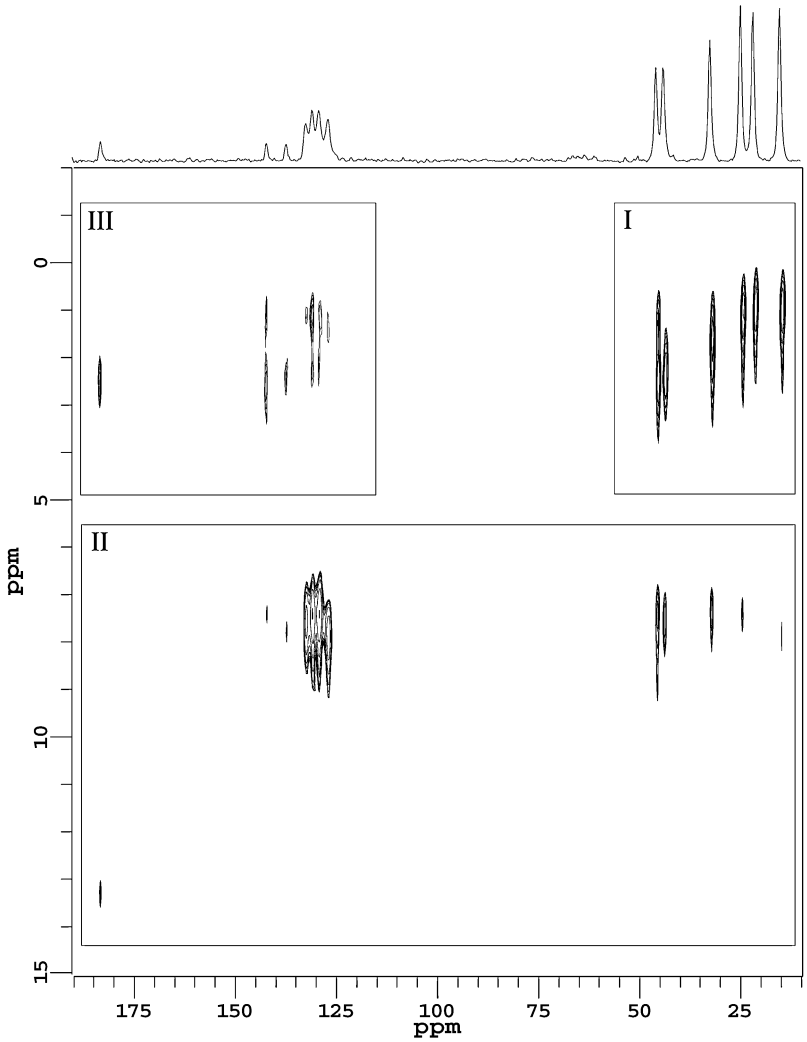

Fig. 7. 2D HETCOR map of IBU-A recorded with a contact time of 300 μs and a spinning rate of 6.600 kHz. The correlation peaks shown in the different regions, labeled by roman numbers in the map, were sampled at different threshold levels for the sake of clarity; the maximum peak intensities (in a.u.) are 100.0 in I, 34.3 in II, and 10.2 in III.

are present. This is not the case in IBU-A, where the two distinct peaks at 22.0 and 25.1 ppm correspond to each of the methyl carbons and can only be explained with the isobutyl group frozen in a well-defined conformation. This is in agreement with reported X-ray (19), neutron diffraction (20), and potential energy calculation (21) studies and also with the 2D correlation experiments described above (i.e., the observed inequivalence between the two methylene protons in IBU-A). By looking at the correlations between the resonances of methyl carbons and those of aromatic protons in the HETCOR experiment, it is also possible to assign the ^{13}C peaks at 25.1 and 22.0 ppm in the IBU-A spectrum to carbons *m* and *n*, respectively, because the more intense correlation peaks shown by the first must be related to a minor distance from the phenyl ring.

A similar situation can be observed for the phenyl signals: the two overlapped signals observed in the IBU-S spectrum at about 130 ppm can be ascribed to the two couples of carbons *d–e* and *f–g* and are indicative of a fast rotation of the phenyl group about its *para* axis. On the contrary, four different resonances can be observed for the tertiary aromatic carbons (from 126.7 to 132.3 ppm) in the room-temperature ^{13}C spectrum of IBU-A.

To get additional information on the occurrence and rate of the interconformational jumps in IBU-A, a series of variable-temperature ^{13}C CP-MAS spectra have been recorded, a selection of which is reported in Fig. 9. Phenyl and isobutyl groups exhibit a quite different behavior. The resonances relative to methyl carbons *m* and *n* do not show any remarkable change at the different temperatures, thus indicating that a sole conformation is populated even at temperatures very close to the melting point (78°C). On the contrary, the resonances ascribable to the tertiary aromatic carbons become increasingly larger by increasing the temperature, and they cannot be any longer distinguished above 40°C, showing the occurrence of peak coalescence. Because in all cases the possibility of line broadening owing to interference between molecular motions and either the MAS rate or the decoupler power (22) has been ruled out by performing experiments at different temperatures, spinning

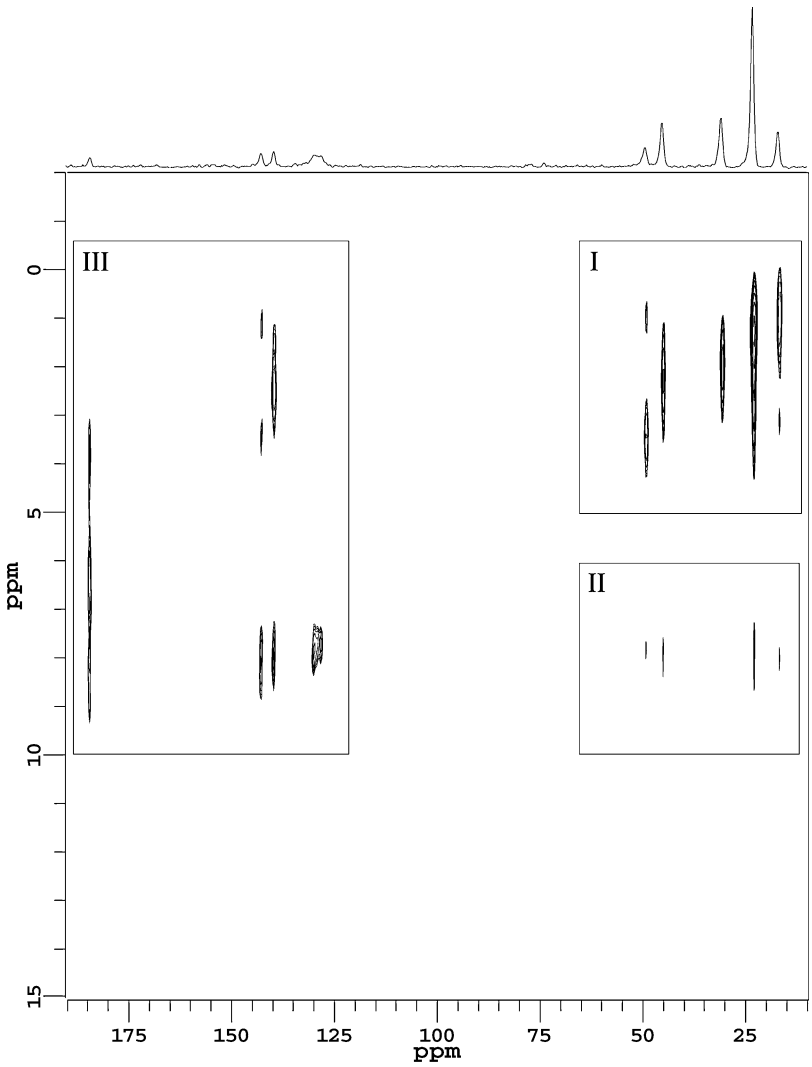

Fig. 8. 2D HETCOR map of IBU-S recorded with a contact time of 300 μs and a spinning rate of 6.600 kHz. The correlation peaks shown in the different regions, labeled by roman numbers in the map, were sampled at different threshold levels for the sake of clarity; the maximum peak intensities (in a.u.) are 100.0 in I, 12.8 in II, and 11.1 in III.

rates, and decoupling conditions, this behavior indicates that the π-ring flip, i.e., the exchange between the two main phenyl conformations, becomes increasingly faster by furnishing thermal energy to the system, and it approaches the intermediate regime (characteristic frequency of the flip of the order of 100 Hz, the difference between the exchanging signals) just below the melting point.

Solid Dispersions

^{13}C Spectra

^{13}C CP-MAS spectra of pure RL and its physical mixtures and coevaporates with each of the two forms of IBU are shown in Fig. 2c–g. The ^{13}C spectrum of RL (Fig. 2c) can be roughly interpreted on the basis of literature data for similar systems (23): ester carbons resonate at about 176 ppm, methyl carbons bound to carbon atoms at 15–20 ppm, and the rest of the carbons in the 35- to 65-ppm region.

The ^{13}C spectra of both the physical mixtures of IBU-A and IBU-S with RL (Fig. 2d and f, respectively) are substantially coincident with the superposition of the ^{13}C spectra of the pure components: this observation strongly suggests that in these solid dispersions, no significant interaction between IBU and RL is present. By the comparison of ^{13}C spectra of IBU-S/RL physical mixture and coevaporate (Fig. 2g), no significant changes in the dynamic and structural behavior of the two components could be detected. This is not the case for the IBU-A/RL coevaporate, the ^{13}C spectrum of which (Fig. 2e) shows remarkable differences with respect to that of the physical mixture. In particular, the aromatic and methyl IBU-A signals are very similar to those present in the ^{13}C spectrum of pure IBU-S and are therefore indicative of the occurrence of fast interconformational dynamics within the isobutyl and phenyl groups. Moreover, the signals of IBU-A appear broader than in the spectrum of the pure drug, because of a larger distribution of isotropic chemical shifts, resulting from

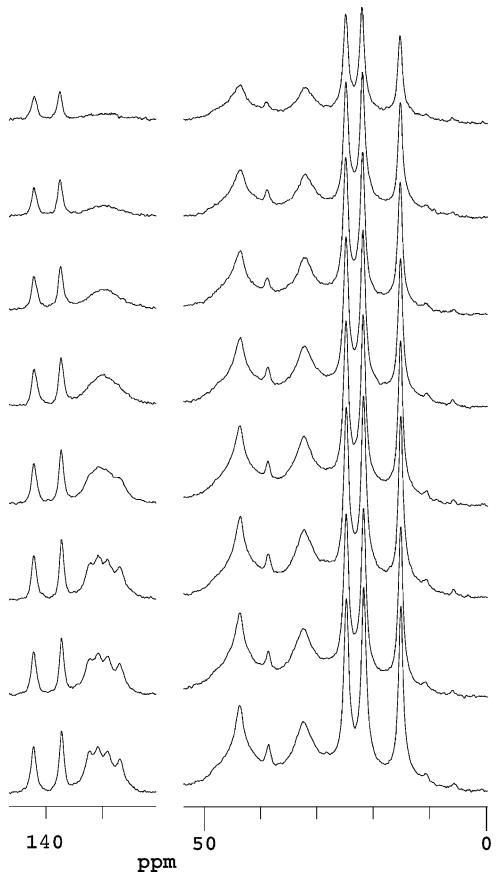

Fig. 9. Variable-temperature ^{13}C CP-MAS spectra of IBU-A recorded from 10 to 70°C (from bottom to top) with a contact time of 1 ms and a spinning rate of 3.5 kHz.

the higher disorder induced by the occurrence of IBU-A/amorphous polymer interactions in the place of the dimeric IBU-A structures. However, together with the methyl signal centered at 23.4 ppm, two smaller resonances at 22.0 and 25.1 ppm can be observed in the spectrum of the IBU-A/RL coevaporate, indicating the presence of small residual crystalline regions of IBU-A, whose dynamic behavior is not modified by the presence of the polymeric matrix, thus not experiencing detectable interactions with this matrix.

These results are in very good agreement with previous PXRD results: in RL-IBU coevaporates prepared at a 33% drug ratio (w/w), both the IBU-A and IBU-S forms gave signals due to drug crystals in PXRD spectra (10). The drug then seemed able to crystallize within the polymer network in the experimental conditions of coevaporation when its concentration exceeded the solubility in the polymer itself. However, a computation of the PXRD data indicated that the residual crystallinity of IBU-S in RL 33% w/w coevaporates is about 3-fold higher than that of IBU-A (10), in agreement with the much stronger modifications induced by the polymer in the molecular structure and dynamics of IBU-A, as highlighted by solid-state NMR.

^1H Spectra

In the ^1H MAS spectrum of RL (see Fig. 4c) three heavily superimposed peaks can be distinguished: the signal at 1 ppm arises from all the aliphatic protons, except those close to the ester groups, giving rise to the large resonance centered at about 3.5 ppm; the narrow peak at the same chemical shift is instead ascribable to the protons of the trimethylammonium groups, the minor line width being in agreement with the fast dynamic processes experienced by these groups.

The ^1H MAS spectra of the two physical mixtures (see Fig. 4d, f) are substantially coincident with the weighted superposition of the ^1H spectra of the single components (taking into account the 1:3 drug-to-polymer ratio), the only exception being represented by a change in the shape of the sharp Eudragit signal at about 3.5 ppm that broadens in both the physical mixtures, probably as a result of a decreased mobility of the trimethylammonium groups. The slight spectral changes occurring in passing from pure components to physical mixtures agree with that already observed from ^{13}C spectra, supporting the conclusion that no significant drug–polymer interactions are present in these solid dispersions.

On the contrary, the ^1H MAS spectra of IBU-A/RL and IBU-S/RL coevaporates (see Fig. 4e and g, respectively) significantly differ from the superposition of the spectra of the pure components. In both cases, the narrow peak at 3.5 ppm not only remarkably broadens, but also shifts to higher frequencies (4.2 and 5.8 ppm for IBU-S and IBU-A coevaporates, respectively), revealing the occurrence of a change in the chemical environment of the trimethylammonium protons, which is particularly strong in the case of IBU-A. Moreover, the acidic proton signal at 12.5 ppm is no longer present in the spectrum of the IBU-A/RL coevaporate, indicating that the IBU acidic group experiences remarkably different interactions with respect to pure IBU-A.

Therefore, we can conclude that the trimethylammonium groups of the polymer are involved in the drug–polymer interactions in the coevaporates of IBU-S and IBU-A, in the latter case interacting with the IBU carboxylic function.

^1H T_1 Measurements

The spin-diffusion process tends to average the spin–lattice relaxation times T_1 of the different protons in a sample to a single value. This average is usually complete when protons belong to the same phase domain, whereas relaxation times of different domains in heterogeneous samples can be completely averaged or not depending on the dimensions of the different domains. This allows information on the mixing degree of different domains on a 100-Å scale to be obtained by measuring ^1H T_1 values (24).

The ^1H T_1 values measured at 20°C for the two pure forms of IBU, RL, and IBU-A/RL solid dispersions are reported in Table III. The T_1's of the pure components are all of the same order of magnitude; in particular, those of IBU-S and RL differ for less than the experimental error, thus preventing us from evaluating the mixing degree between IBU-S and polymer in both their solid dispersions.

In the IBU-A/RL physical mixture the two components maintain relaxation time values quite similar to those measured in the pure samples, thus indicating that in this sample there is no mixing between the two components on a 100-Å scale. On the contrary, a single ^1H T_1 value is measured, within the experimental error, in the IBU-A/RL coevaporate, where drug and polymer are therefore in-

Table III. ^{1}H T_1 Values (in seconds) Determined for Drug and Polymer Components in the Different Samples

	^{1}H T_1 (s)		
	IBU-A	IBU-S	RL
Pure components	1.29 ± 0.04	0.71 ± 0.09	0.78 ± 0.04
IBU-A/RL			
Physical mixtures	1.10 ± 0.09	–	0.81 ± 0.04
Coevaporates	0.83 ± 0.04	–	0.78 ± 0.03

These values were obtained by measuring the relaxation times for each peak in the ^{13}C spectrum and performing an average over all the peaks of the same component.

timately mixed, in full agreement with that previously deduced from ^{13}C experiments.

In Vitro Dissolution Tests

The dissolution curves of IBU from RL coevaporates and physical mixtures were evaluated at room temperature and at different pH values (Fig. 10). The pH 4.5 buffer system was chosen on the basis of the pk_a value of the drug (4.45). In these conditions, the release profile of the drug should be prevalently due to the diffusion across the polymer matrix, with a minimal contribution due to drug dissociation and dissolution. At pH 7.4, the drug is instead highly dissociated and its dissolution rate in the receiving medium would be mainly responsible for drug release. To confirm this hypothesis, a release test was also performed on the IBU-A/RL coevaporate at pH 9.0, at which the drug is totally ionized.

As Fig. 10a shows, IBU release from the IBU-A/RL coevaporate was partial and no difference was seen between pH 4.5 or 7.4, suggesting that the diffusion pathway predominates over the dissolution rate of the drug. Even at the highest pH value (9.0), the release did not exceed 60% of the incorporated drug after 24 h. Such a behavior can be attributed to the formation of strong, although reversible, chemical interactions among the carboxyl groups of drug molecules and the quaternary ammonium heads of the polymer, highlighted by the NMR study discussed above. These results further confirm data previously obtained by us, which indicated that a portion of a carboxylic drug dispersed in an RL matrix can remain associated to the polymer also after several hours of dialysis (7–10). When the physical mixtures were considered, the drug release rate was higher and dependent on the pH of the dissolution medium (Fig. 10a); these findings confirm the absence of a strong association of the drug with RL when the components were simply mechanically mixed.

When the drug was dispersed in RL in its IBU-S dissociated form, the release profile showed that the dissolution properties of the drug affect the rapid leakage from the polymer matrix (Fig. 10b). A "burst" release of 80% of the dispersed drug was registered within 15 min at pH 7.4, confirming that in the salinized form IBU was not able to generate strong interactions with the polymer head groups. At the lower pH, a triphasic profile was observed: i) an initial rapid drug release (40% in 15 min), ii) a *plateau* for the further 8 h of test, followed by iii) a progressive increase of drug release up to 24 h. These phases could be respectively associated with the initial desorption of the drug placed at or near the surface of the coevaporate particles and the following diffusion from within the polymer network after the penetration of the external medium.

In any case, the amount of drug released after 24 h using the IBU-S form greatly exceeded that observed with the acid form and reinforced our hypothesis of a synergistic physical and chemical interaction between Eudragit Retard polymer networks and acidic host molecules. In addition, with this salinized form of the drug, from the physical mixtures the drug release was very fast and unaffected by the polymeric matrix.

CONCLUSIONS

Several ^{1}H and ^{13}C high-resolution solid-state NMR techniques were used to investigate and compare the structural and dynamic behavior of two different forms (acidic and Na salt) of the non-steroidal anti inflammatory

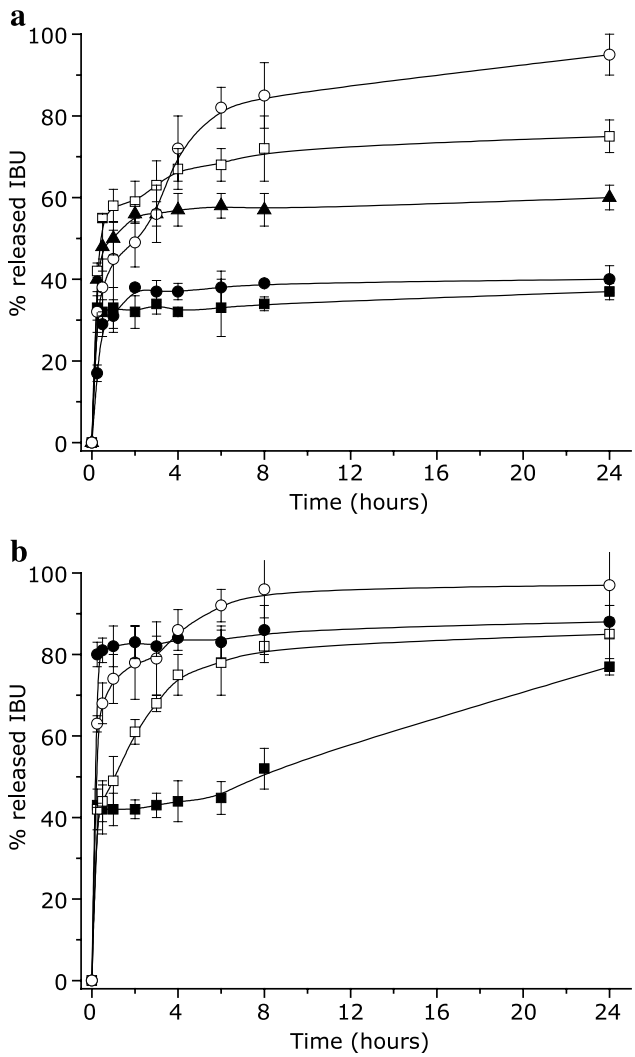

Fig. 10. *In vitro* dissolution curves of IBU from IBU-A/RL (a) and IBU-S/RL (b) coevaporates (filled symbols) and physical mixtures (open symbols), measured at room temperature in different pH buffer solutions (squares, circles, and triangles indicate pH values of 4.5, 7.4, and 9.0, respectively).

drug ibuprofen, as well as of their solid dispersions with the polymer Eudragit RL100, prepared by two different methods (physical mixtures and coevaporates).

Many different high-resolution solid-state NMR techniques (CPPI, FSLG-HETCOR, MAS-J-HMQC, etc.) have been applied to provide a full spectral assignment of ^{13}C resonances, necessary for more detailed structural and dynamic investigations, as well as to determine precise ^{1}H chemical shift values not accessible from simple 1D spectra. In particular, a detailed interpretation of 2D experiments in terms of conformational properties was possible by exploiting structural data from X-ray and neutron diffraction studies and from potential energy calculations already available in the literature.

IBU-A and IBU-S experience quite different dynamic behavior, especially as far as internal motions of molecular fragments are concerned: motional processes of both phenyl (ring flip) and isobutyl (rotation about CH_2–CH bond) groups are fast in the case of IBU-S, whereas they are substantially frozen in IBU-A at room temperature, although phenyl interconformational motions are activated by furnishing thermal energy.

No significant drug–polymer interactions could be observed for the physical mixtures, whereas in the IBU-A/RL coevaporate the two components become intimately mixed at a 100-Å level, and a chemical interaction between the trimethylammonium group of the polymer and the acidic function of ibuprofen could be highlighted from both ^{13}C and ^{1}H spectra. Drug–polymer chemical interactions may also be present in the IBU-S/RL coevaporate at a lower degree, but in this case the only experimental evidences arise from ^{1}H MAS spectra.

The NMR results are in good agreement with *in vitro* dissolution tests, which confirmed that drug release of the IBU-A form from RL matrix is slowed and modulated by the establishment of electrostatic interactions between the components, reinforcing the physical dispersion of the drug within the polymer network.

The structural and dynamic properties of pure IBU in the two forms and of their solid dispersions with RL, as well as the drug–polymer chemical and physical interactions here investigated, should represent an important basis of knowledge for understanding the links between the molecular behavior and the pharmacokinetic/pharmacological properties of the corresponding final drug formulations.

ACKNOWLEDGMENT

Italian MIUR (PRIN 2003) is acknowledged for partial financial support.

REFERENCES

1. S. P. Brown and H. W. Spiess. Advanced solid-state NMR methods for the elucidation of structure and dynamics of molecular, macromolecular, and supramolecular systems. *Chem. Rev.* **101**:4125–4155 (2001).
2. R. K. Harris. Polymorphism and Related Phenomena. In D. M. Grant and R. K. Harris (eds.), *Encyclopedia of NMR, Vol. 6, Wiley,* Chichester, 1996, pp. 3734–3740.
3. P. A. Tishmack, D. E. Bugay, and S. R. Byrn. Solid state nuclear magnetic resonance spectroscopy—pharmaceutical applications. *J. Pharm. Sci.* **92**:577–610 (2003).
4. S. R. Vippagunta, H. G. Brittain, and D. J. W. Grant. Crystalline solids. *Adv. Drug Deliv. Rev.* **48**:3–26 (2001).
5. D. E. Bugay. Characterization of the solid state: spectroscopic techniques. *Adv. Drug Deliv. Rev.* **48**:43–65 (2001).
6. D. M. Schachter, J. Xiong, and G. C. Tirol. Solid state NMR perspective of drug–polymer solid solutions: a model system based on poly(ethylene oxide). *Int. J. Pharm.* **281**:89–101 (2004).
7. R. Pignatello, M. Ferro, G. De Guidi, G. Salemi, M. A. Vandelli, S. Guccione, M. Geppi, C. Forte, and G. Puglisi. Preparation, characterisation and photosensitivity studies of solid dispersions of diflunisal and Eudragit RS100® and RL100®. *Int. J. Pharm.* **218**:27–42 (2001).
8. R. Pignatello, M. Ferro, and G. Puglisi. Preparation of solid dispersions of nonsteroidal anti-inflammatory drugs with acrylic polymers and studies on mechanisms of drug–polymer interaction. *AAPS PharmSciTech* **3**:10 (2002).
9. R. Pignatello, C. Bucolo, P. Ferrara, A. Maltese, A. Puleo, and G. Puglisi. Eudragit RS100® nanosuspensions for the ophthalmic controlled delivery of Ibuprofen. *Eur. J. Pharm. Sci.* **16**:53–61 (2002).
10. R. Pignatello, D. Spadaro, M. A. Vandelli, F. Forni, and G. Puglisi. Characterization of the mechanism of interaction in ibuprofen–Eudragit RL100 coevaporates. *Drug Dev. Ind. Pharm.* **30**:277–288 (2004).
11. F. H. Allen and O. Kennard. 3D search and research using the Cambridge Structural Database. *Chem. Des. Autom. News* **8**: 31–37 (1993).
12. F. H. Allen. The Cambridge Structural Database: a quarter of a million crystal structures and rising. *Acta Crystallogr. B* **58**:380–388 (2002).
13. I. J. Bruno, J. C. Cole, P. R. Edgington, M. Kessler, C. F. Macrae, P. McCabe, J. Pearson, and R. Taylor. New software for searching the Cambridge Structural Database and visualizing crystal structures. *Acta Crystallogr. B* **58**:389–397 (2002).
14. W. D. Dixon. Spinning-sideband-free and spinning-sideband-only NMR spectra in spinning samples. *J. Chem. Phys.* **77**:1800–1809 (1982).
15. X. Wu and K. W. Zilm. Methylene-only subspectrum in CPMAS NMR. *J. Magn. Reson.* **104**:119–122 (1993).
16. A. Lesage, D. Sakellariou, S. Steuernagel, and L. Emsley. Carbon-proton chemical shift correlation in solid state NMR by through-bond multiple-quantum spectroscopy. *J. Am. Chem. Soc.* **120**:13194–13201 (1998).
17. B. J. Van Rossum, H. Forster, and H. J. M. De Groot. High-field and high-speed CP-MAS^{13}C NMR heteronuclear dipolar—correlation spectroscopy of solids with frequency-switched Lee–Goldburg homonuclear decoupling. *J. Magn. Reson.* **124**: 516–519 (1997).
18. R. Kitamaru, F. Horii, and K. Murayama. Phase structure of lamellar crystalline polyethylene by solid-state high-resolution carbon-13 NMR detection of the crystalline–amorphous interphase. *Macromolecules* **19**:636–643 (1986).
19. J. F. McConnell. 2-(4-Isobuthylphenyl) propionic acid. $C_{13}H_{18}O_2$ ibuprofen or prufen. *Cryst. Struct. Commun.* **3**:73–75 (1974).
20. N. Shankland, C. C. Wilson, A. J. Florence, and P. J. Cox. Refinement of ibuprofen at 100 K by single-crystal pulsed neutron diffraction. *Acta Crystallogr. C* **53**:951–954 (1997).
21. N. Shankland, A. J. Florence, P. J. Cox, C. C. Wilson, and K. Shankland. Conformational analysis of Ibuprofen by crystallographic database searching and potential energy calculation. *Int. J. Pharm.* **165**:107–116 (1998).
22. W. P. Rothwell and J. S. Waugh. Transverse relaxation of dipolar coupled spin systems under rf irradiation: detecting motions in solids. *J. Chem. Phys.* **74**:2721–2732 (1981).
23. C. Forte, M. Geppi, S. Giamberini, G. Ruggeri, C. A. Veracini, and B. Mendez. Structure determination of clay/methyl methacrylate copolymer interlayer complexes by means of ^{13}C solid state n.m.r. *Polymer* **39**:2651–2656 (1998).
24. L. Calucci, L. Galleschi, M. Geppi, and G. Mollica. Structure and dynamics of flour by solid state NMR: effects of hydration and wheat aging. *Biomacromolecules* **5**:1536–1544 (2004).